

X-irradiation-induced cell cycle delay and DNA double-strand breaks in the murine osteoblastic cell line OCT-1

Patrick Lau · Christa Baumstark-Khan ·
Christine E. Hellweg · Günther Reitz

Received: 9 December 2008 / Accepted: 16 February 2010 / Published online: 16 March 2010
© Springer-Verlag 2010

Abstract Radiation response of bone cells, especially the bone-forming osteoblasts, is an important issue for radiotherapy in young age. A radiation-induced cell cycle arrest may enhance or accelerate osteoblastic differentiation. To analyze radiation response of osteoblastic cells, the correlation between DNA double-strand break induction (DSB), cell cycle alterations and gene expression modifications after X-irradiation was investigated in the osteoblast-like cell line OCT-1. As marker of the cellular response to DSB, the temporal appearance of γ -H2AX foci after X-irradiation was visualized. Gene expression profiles of the key cell cycle regulatory protein p21 (CDKN1A), and the most abundant growth factor in human bone, transforming growth factor beta 1 (TGF- β 1) were recorded using quantitative real-time reverse transcription PCR (qRT-PCR). The distribution of cells in the cell cycle phases G1, S and G2 was determined by propidium iodide (PI) staining and flow cytometry. Initial studies show a strong dose dependency in the number of γ -H2AX foci shortly after X-irradiation. Exposure to 1 Gy yields approximately 36 small foci in OCT-1 cells after 30 min that became larger after 1 h of incubation; after 24 h most of the foci had disappeared. X-rays provoked a dose-dependent arrest in G2 phase of the cell cycle, accompanied by a dose-dependent gene expression regulation for p21 and TGF- β 1. As TGF- β 1 is known to affect osteoblast differentiation, matrix formation and mineralization, modulation of its expression could influence the expression of the main osteogenic transcription factor Runx2 (Cbfa1) and other osteoblast differentiation markers.

Abbreviations

ALP	Alkaline phosphatase
BSA	Bovine serum albumin
DAPI	4, 6-diamidino-2-phenylindole
DSB	Double-strand break
qRT-PCR	Quantitative real-time reverse transcription polymerase chain reaction
PBS	Phosphate-buffered saline
PI	Propidium iodide
RT	Reverse transcriptase

Introduction

Bone mass in mammals is governed by the bone-specific remodeling process. This comprises the balanced action of osteoblasts, the skeletal cells that are responsible for synthesis, deposition and mineralization of extracellular matrix of bone (Aubin 1998) and of osteoclasts, the hematopoietic lineage-derived cells that are capable of bone resorption (Augat et al. 2005; Strewler 2004). Apart from producing extracellular matrix, the osteoblasts synthesize cytokines and activation factors allowing them to communicate with osteoclasts (zur Nieden et al. 2003). Osteogenic cells arise from multipotential mesenchymal cells that have the capacity to undergo a number of apparently stochastic commitment or restriction steps to give rise to progeny with more limited, including monopotent capacities (Aubin et al. 1995). The sequential process of osteoblastic differentiation includes a phase of cell proliferation, followed by coordinated expression of bone-related proteins (Stein and Lian 1993). The differentiation of osteoblastic precursor cells into osteoblasts is controlled by a bunch of specific transcription factors of which Runx2 (also known as core binding factor alpha 1 (Cbfa1)) is the most important one. Most

P. Lau · C. Baumstark-Khan (✉) · C. E. Hellweg · G. Reitz
Division of Radiation Biology, Institute of Aerospace
Medicine, German Aerospace Center (DLR),
Linder Höhe, 51147 Köln, Germany
e-mail: christa.baumstark-khan@dlr.de

of the specific genes coding for the osteoblast lineage contain binding sites in their promoter regions for the Runx2 gene product and are thus up-regulated upon Runx2 induction (Ducy et al. 1997; Harada et al. 1999; Kern et al. 2001). Runx2 directs mesenchymal progenitor cells toward pre-osteoblasts and inhibits their differentiation into adipocytes and chondrocytes (Komori 2006). Another key regulator of cell proliferation, differentiation, motility and apoptosis is transforming growth factor beta1 (TGF- β 1) (Kanaan and Kanaan 2006), a secreted factor present at high levels in bone. TGF- β 1 is a homodimeric protein with autocrine and paracrine activities, found in a variety of cell types (Roberts and Sporn (1993). TGF- β is produced and incorporated into the mineralized bone matrix by osteoblasts and inhibits osteoclast proliferation and activity. Moreover, it stimulates proliferation and differentiation of pre-osteoblasts (Langdahl et al. 2003) and inhibits the mineralization process e.g. in mouse osteoblastic MC3T3-E1 cells (Sowa et al. 2002). Recent observations suggest that TGF- β 1 inhibits terminal osteoblast differentiation by repressing the transcriptional activity of Runx2, which prevents the appearance of mature osteoblasts (Alliston et al. 2001; Komori et al. 1997; Otto et al. 1997). The inhibition of differentiation is mediated via Smad3, which interacts with Runx2 and represses transcriptional activity (Kanaan and Kanaan 2006). Smad3-mediated repression of Runx2 provides a central regulatory mechanism for the inhibition of osteoblast differentiation by TGF- β 1, since it inhibits both, Runx2 transcription and transcriptional activation of osteoblast-specific marker genes like the vitamin K- and vitamin D-dependent matrix protein osteocalcin (Alliston et al. 2001).

Modulations in gene expression patterns during the differentiation process give rise to the question whether the differentiation process affects the cellular response to DNA-damaging agents like ionizing radiation and whether IR affects the osteoblast-specific differentiation process. Ionizing radiation produces a wide spectrum of molecular lesions in DNA including base damages, single-strand breaks (SSB), double-strand breaks (DSB), as well as multiply damaged sites. However, DSB are the most relevant lesions for cell killing as they disrupt both DNA strands in close proximity (Rothkamm and Löbrich 2003). Cellular recognition of DSB and their efficient repair is therefore of utmost importance. Otherwise, if these lesions are left unrepaired, basic cellular functions may be impaired, resulting in reduced cell survival. DNA in eukaryotes is packaged along with core histone proteins into a fundamental subunit of the chromosome, the nucleosome. H2A is one of the core histone families that have been conserved throughout evolution. This mammalian subfamily has a histone variant, known as H2AX (Rogakou et al. 1998). After exposure to ionizing radiation, H2AX is phosphorylated at serine 139

within its conserved COOH-terminal region in the vicinity of DSB sites. The number of such phosphorylated γ -H2AX foci correlates well with the number of DSB (Rothkamm and Löbrich 2002).

In a number of soft tissues, cells respond to high doses of radiation by the induction of necrosis, while lower doses induce apoptosis (Szymczyk et al. 2004). The deleterious effect of ionizing radiation on growing human bone is well documented (Hopewell 2003). A series of in vivo studies on the effects of radiation on bone have been reported (Probert and Parker 1975; Goldwein 1991; Arnold et al. 1995), but the effects of ionizing radiation on the bone-forming osteoblastic cells themselves still remain obscure (Dare et al. 1997). Exposure to 20 Gy of X-rays reduced osteoblastic cell proliferation, followed by a decreased collagen production and alkaline phosphatase (ALP) activity (Sams 1965). Since both collagen production and ALP activity play major roles in the differentiation process of non-mineralized bone, it has been proposed that the reduced expression paves the pathway to osteopenia (Erguen and Howland 1980). In addition, cell death of osteocytes and osteoblasts could contribute in the pathogenesis of osteoradionecrosis (Dudziak et al. 2000). Recent studies suggest that ionizing radiation affects immature more than mature bone, supporting the classic proposition that pre-osteoblasts are radiosensitive (Jacobsson et al. 1985, 1986; Tonna and Pavelec 1970). To better understand the effects of ionizing radiation on osteoblasts and to assess the possibility of detrimental effects of ionizing radiation on bone formation, we investigated the effect of radiation on cell cycle progression and expression of osteoblastic marker genes, which are important players in the differentiation process. In the present paper, we show that ionizing radiation induces dose-dependent modulation in cell cycle progression. These results suggest that exposure to higher doses of ionizing radiation inhibits cell cycle progression leading to modulations in osteoblast-specific gene expression.

Materials and methods

Cell lines and culture conditions

The murine osteoblast precursor cell line OCT-1 (Chen et al. 1995) was maintained at 37°C in a humidified atmosphere of 5% CO₂ and 95% air. The culture medium was replenished every 3–4 days. Standard culture medium was used for cell maintenance. For that, cells were inoculated at a cell density of 5×10^3 cells per cm² and maintained in α -modified Eagle's medium (α -MEM, Gibco, Paisley, UK), supplemented with 10% fetal bovine serum (FBS; Biochrom GmbH, Berlin). For differentiation experiments, the

cells were incubated in Petri dishes (\varnothing 10 cm) or well plates and cultivation was continued for up to 14 days after irradiation. The medium was replenished twice per week.

Irradiation procedure

After an initial growth period of 2–3 days, asynchronous actively proliferating OCT-1 cells were exposed to X-rays (150 kV, 16 mA) at a dose rate of 1.8 Gy/min (focus-object distance of 312 mm) using the X-ray source Müller Typ MG 150 (MCN 165, Philipps, Hamburg, Germany). Control cells were treated similarly but without X-ray exposure.

Colony formation assay

For survival experiments, cells were irradiated attached to Petri dishes (\varnothing 6 cm) at cell densities adjusted to compensate for cloning efficiency of the cell lines and any anticipated lethal effect of the radiation, in order to obtain between 50 and 100 colonies per culture dish. Cells were further incubated at 37°C immediately after irradiation for 14–20 days. The grown colonies were fixed with 1% formaldehyde and stained with 0.1% (w/v) crystal violet solution. Colonies consisting of more than 50 cells were scored as “survivors”. The survival rate of the irradiated cells was normalized to the plating efficiency of non-irradiated controls. All data of the irradiated samples were compared using the *t*-test and fit by least squares linear regression analysis to $\ln S_D/S_{D=0}$ versus dose, where S_D and $S_{D=0}$ were the surviving fractions of irradiated and non-irradiated cells, respectively. The resulting dose–effect curve, described by the formula $S = 1 - (1 - \exp^{-D/D_0})^n$, was characterized by the parameters D_0 and n (single hit multitarget model) (Hug and Kellerer 1966). Survival results were averaged data from three independent experiments.

Detection of γ -H2AX foci

Cells were grown on glass coverslips (\varnothing 11 mm), exposed to X-rays and incubated under standard conditions for various time points to allow damage repair. Cells on cover slips were fixed in 3.5% formaldehyde in PBS for 30 min, rinsed three times in PBS for each 10 min, permeabilized for 30 min on ice in 0.5% Triton X-100 in PBS with 1% BSA and blocked in PBS with 1% bovine serum albumin for 10 min. Cells were incubated for 1 h with purified rabbit anti-phospho-histone H2AX (S139) antibody (AF2288, R&D Systems) diluted 1:400 in 1% FCS in PBS, and washed three times in PBS containing 1% bovine serum albumin for 10 min each time. Cover slips were rinsed and incubated with fluorescent secondary TRITC-conjugated polyclonal swine anti-rabbit (Dako Cytomation, Glostrup, Denmark) antibody in 1% FCS in PBS diluted 1:250 for 1 h

at room temperature in the dark. DNA was counterstained using $1 \mu\text{g ml}^{-1}$ 4',6-diamidino-2-phenylindole (DAPI), and cover slips were mounted using Dako fluorescent mounting medium (Carpinteria, California, USA). Cellular red (TRITC) and blue (DAPI) fluorescence emissions of identical cells were visualized and documented using standard filter settings (for TRITC filter set 20: excitation at $\lambda = 546$ nm, emission at $\lambda = > 575$ nm; for DAPI filter set 2: excitation at $\lambda = 365$ nm, emission at $\lambda = > 420$ nm). For quantitative two-dimensional analysis during the imaging process, foci were counted automatically and resulting counts were controlled by eye using a 63 \times objective on a Zeiss fluorescence microscope (Carl Zeiss Inc., Thornwood, NY) equipped with Axio vision software 4.0 (Zeiss Thornwood, NY) and recorded on a AxioCam MRm5 Rev.3 (Carl Zeiss Inc., Thornwood, NY), equipped with a CCD imaging system. In a single experiment, 100 cells were analyzed and counted per sample. Control experiments were sham-irradiated in all experiments.

Cell cycle analysis

Cells were initially plated at a density of (5×10^3 cells/cm²) in Petri dishes (\varnothing 6 cm) and grown for 2 days to allow irradiation in exponential growth phase. Cells were harvested at the indicated time points by gentle trypsinization followed by immediate fixation in 70% ice-cold ethanol with an overnight incubation at -20°C . The ethanol was removed by dilution with PBS and brief centrifugation (500 \times g). Thereafter, pelleted cells were washed once with PBS and incubated for 30 min at 37°C in PBS containing 40 $\mu\text{g ml}^{-1}$ of propidium iodide (Sigma–Aldrich, Steinheim, Germany) and 10 $\mu\text{g ml}^{-1}$ of DNase-free RNase (Sigma–Aldrich). For each tube, 20,000 cells were immediately measured on a FACScan flow cytometer (Becton–Dickinson) using CellQuest Pro Software.

Quantitative real-time reverse transcriptase polymerase chain reaction (qRT–PCR)

Changes in gene expression of the bone-specific differentiation process after irradiation was analyzed in OCT-1 cells. To get a profile of gene expression during the initial phases of osteoblastic differentiation (proliferation phase), RNA was harvested for analysis from 0 to 7 days after irradiation.

The examination of gene expression profiles was performed using quantitative polymerase chain reaction (qPCR) technique, after reverse transcription of the RNA. Total cellular RNA was isolated using the RNeasy Mini kit (Qiagen, Hilden, Germany) according to the manufacturer's specifications. DNase treatment was performed on column using RNase-free DNase kit (Qiagen, Hilden, Germany). The integrity of RNA was assessed using

lab-on-chip Bioanalyzer 2100 (Agilent Technologies, USA). Only samples with RNA integrity numbers (RIN) higher than eight were used for downstream applications (Fleige and Pfaffel 2006). First strand cDNA was synthesized from 500 ng total RNA using the iScript reverse transcriptase RNase H⁺ (BioRad, CA), containing oligo (dT) and random hexamer primers according to the manufacturer (BioRad) in a final volume of 20 μ l. Gene-specific forward and reverse primer pairs were purchased from Qiagen (<http://www.qiagen.com/GeneGlobe>) containing gene sequences derived from the NCBI Reference Sequence database (<http://www.ncbi.nlm.nih.gov/RefSeq>). Primers are validated to detect RNA only and provided that no pseudogenes with high cDNA similarity exist or that the transcript is not derived from a single-exon gene. Primers were purchased for the target genes Cyclin-dependent kinase inhibitor 1A (P21) p21(WAF/CDKN1a), Transforming growth factor beta 1 (TGF- β 1), Runx2 (Cbfa1), and for the house-keeping genes Beta-2-microglobulin (B2M), Hypoxanthine guanine phosphoribosyl transferase (HPRT), TATA box binding protein (TBP). PCR conditions were optimized and standard curves were generated. All qPCRs were performed using SYBR Green-based detection using the DNA Engine Opticon2 System (BioRad Ltd, Munich, Germany). The authenticity of the PCR products was verified using melting curve analysis and agarose gel electrophoresis.

For qPCRs, a ready to use cocktail containing 12.5 μ l 2 \times Green RT-PCR (Platinum SYBR Green qPCR Super-Mix-UDG, Invitrogen), 0.5 μ l forward primer (Qiagen), 0.5 μ l reverse primer (Qiagen) and 2 μ l cDNA template were used in a final volume of 20 μ l. After an initial 50°C step for 2 min (UDG incubation) and denaturation of 2 min at 95°C followed 40 cycles of 15 s at 95°C, 30 s at 60°C and 30 s at 72°C. The detection of fluorescence signals was performed at 72°C at each cycle. C_t (threshold cycle) values were calculated using the Opticon-2 software. For each primer set the non-template controls and the RT-negative control samples were analyzed in addition to the non-treated and treated samples. Housekeeping genes were chosen according to the fact that they belong to different functional and abundance classes in various tissues and cells with various but stable levels in gene expression. Due to the fact that no gene is constantly expressed, multiple housekeeping genes are required for an accurate normalization (Vandesompele et al. 2002).

Quantification of gene expression was based on the C_t value for each sample. The C_t values were calculated as the average of triplicate measurements. Relative quantification was performed including measurement of the difference in copy numbers between two samples that have each been normalized to an endogenous reference gene (“housekeeping gene”). This method does not rely on the knowledge of a given transcript copy number in a standard sample. Instead, the changes in gene expression levels of a specified

transcript may be measured and described in arbitrary unit relative to the level of some other control transcript in the same sample pool. This method referred to as efficiency-corrected ΔC_t method builds upon the relative standard curve method by incorporating PCR efficiency (E) into the quantity calculation (Nolan et al. 2006). The PCR efficiency was evaluated from dilution series of purified PCR products. The standard curve slopes are used to calculate PCR efficiency according to the relationship $E = 10^{(-1/\text{slope})}$ as described (Rasmussen 2001).

Relative expression levels of all investigated genes were determined using pair wise fixed reallocation randomization test (REST) software (Pfaffl 2001; Pfaffl et al. 2002). Normalization of target gene expression to the optimal combination of housekeeping gene expression is achieved using the BestKeeper software (Pfaffl et al. 2004).

Determination of bone cell differentiation by von Kossa staining of mineralized nodules

The main characteristic of mature bone cells is their ability to deposit extracellular matrix that mineralizes (Aubin 1998). Under in vitro culture conditions, the deposited calcium co-precipitates with phosphate to form bone nodules (Chentoufi et al. 1993), which can be assessed using von Kossa staining method. Mineralization of OCT-1 cells was determined 14 days after irradiation. For that, cells were fixated with 1% formaldehyde (Sigma–Aldrich, Taufkirchen, Germany) buffered with 10 mM phosphate (pH 6.9) at 4°C for 30 min followed by staining with 0.5 ml of 5% silver nitrate solution for 30 min. Exposure to UV-C light for 10 min at room temperature leads to the deposition of silver by replacing the reduced calcium. After treatment with 2.5% sodium thiosulfate for 5 min (to remove unreacted silver), the cells were rinsed twice with distilled water. Under the microscope, mineralized bone nodules show dark brown to black staining while non-mineralized areas display only light brown staining.

Results

The immortalized murine bone cell line OCT-1 was used to study the differentiation process of osteoblast-like cells after exposure to ionizing radiation. The use of this cell line that is capable of differentiating along the bone cell lineage provides an excellent model for studying patterns of gene expression in differentiating osteoblasts.

Survival after X-irradiation

The colony-forming ability after X-ray treatment was investigated to determine the survival rate of the OCT-1

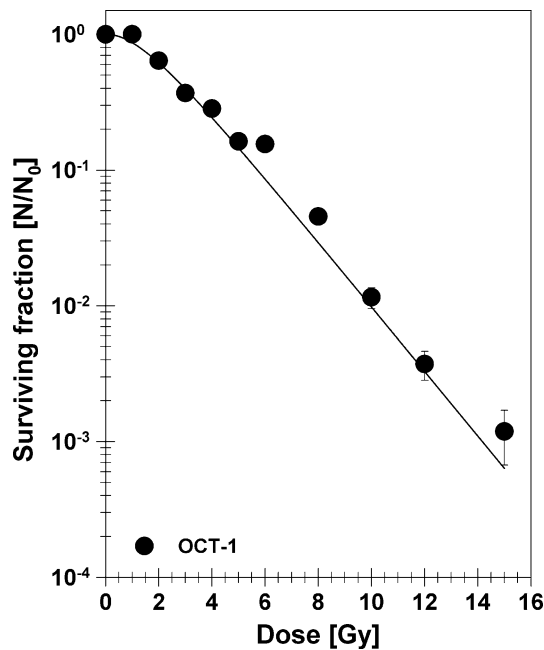


Fig. 1 Dose–effect relationship after exposure to ionizing radiation. OCT-1 cells were exposed to ionizing radiation up to 15 Gy. The colony-forming ability after X-ray treatment was investigated to determine the survival rate of the cell line

cell line. The cells were irradiated in a dose range from 0 to 15 Gy. The OCT-1 cells have the capability to recover from DNA damage as the dose–effect curve (Fig. 1) is of curvilinear shape with a shoulder in the low dose range and an exponential curve progression in the high dose range. Survival was determined to be connected to dose via the characteristic parameters D_0 and n . The D_0 for OCT-1 cells lies with a value of 1.83 ± 0.05 in the range published for human mesenchymal-derived fibroblast cell lines, the same is true for the n -value of 2.35 ± 0.26 . The shoulder width is described by a quasi-threshold dose of 2.6 Gy.

Detection of γ -H2AX foci

The analysis of γ -H2AX focus formation was done to investigate the induction and repair of DSB after exposure to ionizing radiation (1 Gy). By subsequent immune staining using antibodies against γ -H2AX, discrete foci were detected inside the cell nuclei (Fig. 2). Foci formation was additionally examined in non-irradiated control cells. After exposure to 1 Gy, discrete foci were microscopically visible as early as 30 min after irradiation. After a repair period of 24 h, nearly all DSB were effectively rejoined (Fig. 3).

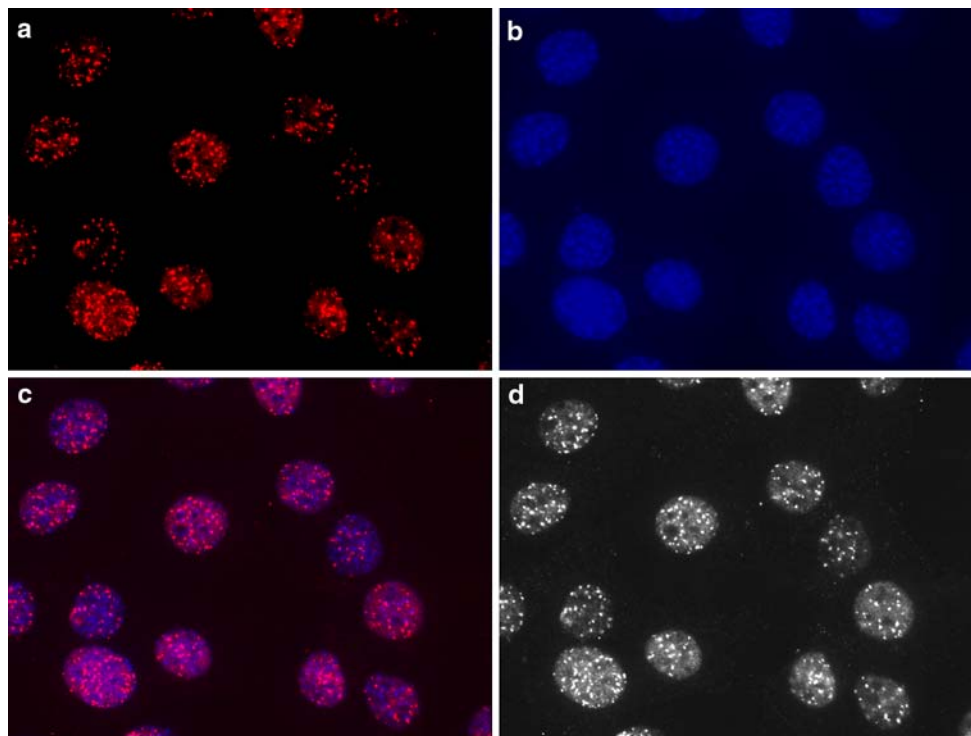


Fig. 2 DSB induction in murine bone cell line OCT-1 as measured by γ -H2AX focus formation 30 min after 1 Gy of X-irradiation. γ -H2AX-TRITC-fluorescence as visualized in the Zeiss fluorescence microscope using filter set 20 at an emission at $\lambda > 575$ nm (a); DNA

counterstained with DAPI as visualized in the Zeiss fluorescence microscope using filter set 2 at an emission at > 420 nm (b); image resulting from merging both channels using the Axio vision software 4.0 (c) and monochrome image of the merged image (d)

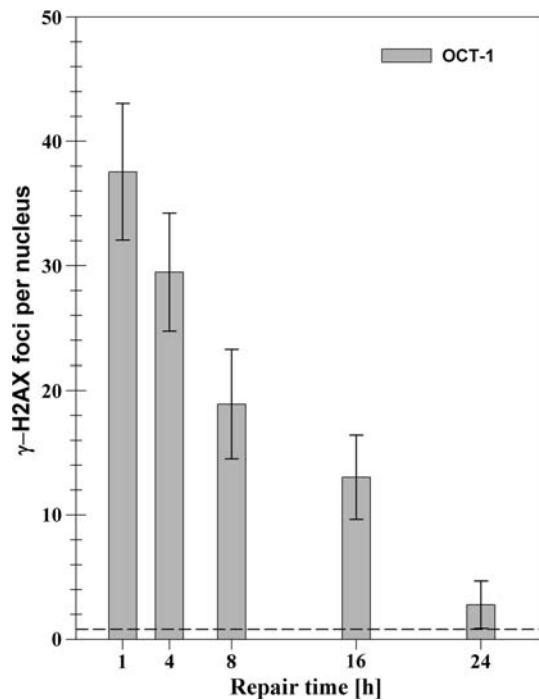


Fig. 3 Decay of γ -H2AX foci with repair time. Exposure to 1 Gy yields about 36 small foci that were already visible after 30 min and fully developed after 1 h. With increasing repair time, the number of foci decreased exponentially. At 24 h of repair, only about 3 foci were present. A total of 100 cells were analyzed to obtain the mean and standard derivation. The *dashed line* represents the number of foci in unirradiated cells

Cell cycle distributions

Modulations in cell cycle distribution were examined using propidium iodide staining and flow cytometry analysis. The present study demonstrated that ionizing radiation at a dose range between 2 and 7 Gy induced a dose- and time-dependent cell cycle arrest in OCT-1 cells. The flow cytometry data indicates that 8 h after exposure to 4 Gy, a significant increase in G2-arrested cells were detected. However, 7 Gy arrested almost the entire cell population (Fig. 4). After an incubation time of 48 h, a considerable fraction of cells seemed to have started cycling again, as documented by the appearance of S-phase signals.

X-ray-induced modulation of gene expression

In this study, we evaluated the effects of ionizing radiation on the expression of key transcription factors, cell cycle regulators and genes that are directly linked to the osteoblastic cell differentiation and maturation process like the osteoblast-specific transcription factor Runx2, p21 and TGF- β 1. Exposure to ionizing radiation increased the expression of the cell cycle regulator p21 in a dose-dependent manner 8 h after exposure (Fig. 5a). Seven days after

radiation exposure, the expression level reached the control level. Irradiation decreased Runx2 expression level immediately after exposure to ionizing radiation considerably (Fig. 5b). For lower radiation doses (2 and 4 Gy), Runx2 expression levels reached control levels. Seven Gy, however, provoked a significant up-regulation of Runx2 reaching a maximum expression level after 3 days post-exposure. After exposure to ionizing radiation, the TGF- β 1 expression levels are dose-dependently up-regulated, peaking at 24 h after X-ray treatment. Seven days after exposure, the expression levels for all radiation doses reached the control level (Fig. 5c).

X-ray-induced differentiation along the bone cell lineage

To determine X-ray-induced premature differentiation of the OCT-1 cell line, mineralized bone nodules were stained with the von Kossa method, which demonstrates deposits of calcium or calcium salt during bone cell differentiation. Figure 6 shows a bright-field microscopic view of cells grown for 14 days after irradiation. The non-irradiated cells (Fig. 6a) display only a light to intermediate gray staining, while the irradiated cells stain darker.

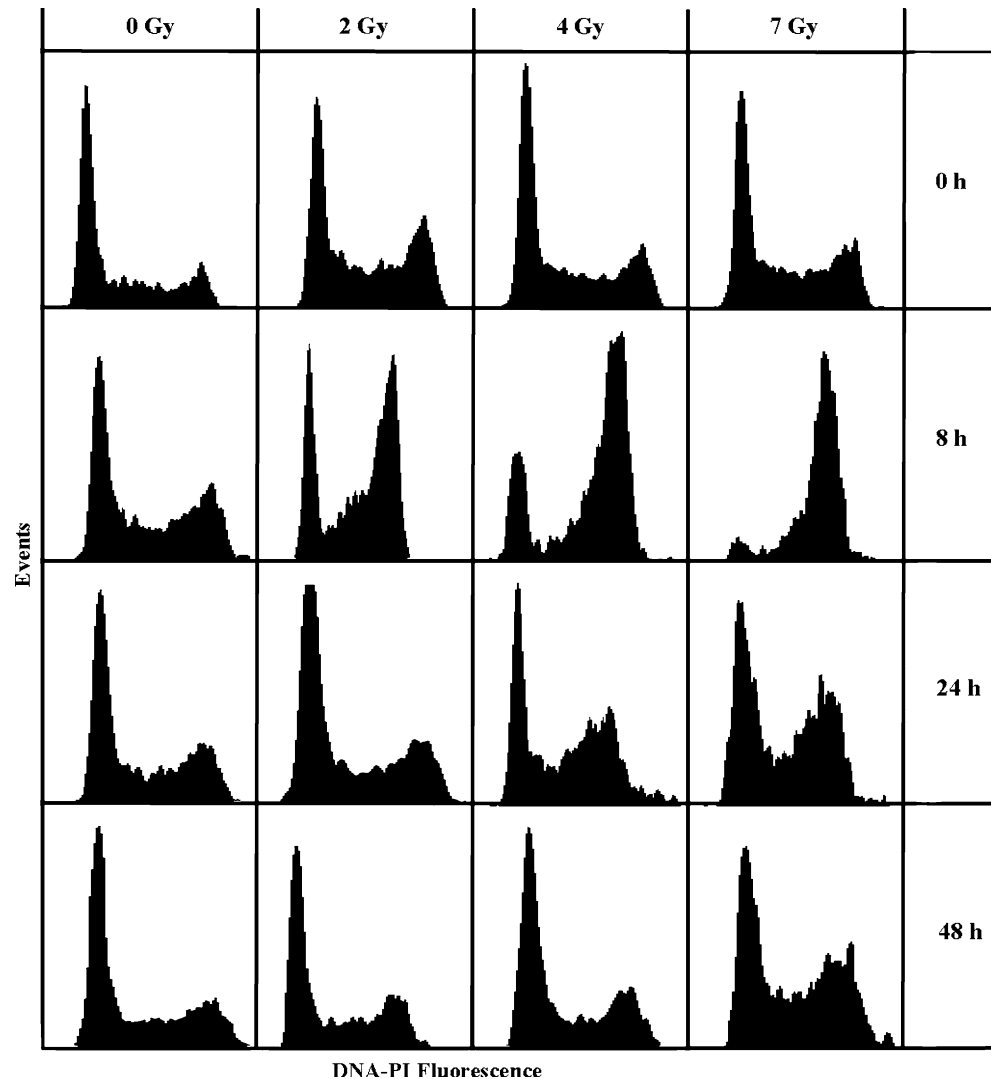
For cells irradiated with 2 Gy (Fig. 6b), small black-staining bone nodules are formed. After irradiation with 4 Gy (Fig. 6c), discrete calcium-containing bone nodules were formed. For cells irradiated with 7 Gy of X-rays (Fig. 6d), sites of calcium deposition increase in size and number.

Discussion

During early differentiation, bone-forming osteoblasts undergo a complex developmental process consisting of the initial recruitment and proliferation of osteoblastic precursor cells (Aubin 1998). Terminal differentiation is achieved either intrinsically through a specific number of cell divisions (Hayflick 1965; Rodemann et al. 1989) or prematurely by exposure to various types of stress, including ultraviolet light (Mass et al. 2003) as well as X-rays (Herskind et al. 2000; Herskind and Rodemann 2000; Fournier et al. 2001). Irradiation as well as exposure to toxic agents that cause DNA damage, such as cancer chemotherapeutics, usually inhibit cell proliferation by activating cell cycle checkpoint functions and causing growth arrest at specific cell cycle phases (Zhou et al. 2007).

To investigate the effects of radiation on the bone cell line OCT-1 in detail, we analyzed the relationship between cell cycle modulations and the initiation of the osteoblast-specific differentiation process in connection to modulation of osteoblast-specific gene expression patterns after exposure to IR.

Fig. 4 Cell cycle progression of OCT-1 cells after irradiation with 0, 2, 4 and 7 Gy



The investigated murine calvaria-derived bone cell line OCT-1 has been reported to be capable of differentiating along the osteoblast lineage (Chen et al. 1995). Originally, OCT-1 cells were isolated from a transgenic mouse carrying the SV 40 large T antigen under control of a bone-specific osteocalcin gene (Chen et al. 1995). Thus, OCT-1 cells obviously represent an early stage of the osteoblast lineage and can serve as a useful *in vitro* model for studying the developmental differentiation process from pre-osteoblastic precursor cells to mature osteoblasts.

To investigate the molecular mechanism underlying radiation-triggered differentiation of pre-osteoblasts into mature osteoblasts, we analyzed the cellular response of OCT-1 cells to IR. The progressive development of the osteoblastic phenotype requires a precise coordination between cellular proliferation and differentiation. The induction of DSB by irradiation is known to be not only the cause of mutations, neoplastic transformation, and reproductive cell death, but also of accelerated senescence

(Suzuki et al. 2001) and pre-mature differentiation in human fibroblasts (Herskind et al. 2000; Herskind and Rodemann 2000; Fournier et al. 2001). This might be considered to be a cellular survival strategy when radiation damage is not sufficiently repaired and the integrity of the genome can not be maintained.

In the current paper, we investigate the effects of ionizing radiation on DSB induction and repair, cell cycle progression and expression of osteoblastic marker genes that are important players in the differentiation process. Differentiation is visualized by staining bone nodules formed by deposition of extracellular matrix and calcium.

Our results indicate that the investigated murine osteoblastic cell line OCT-1 displays sensitivity toward ionizing radiation comparable to that of human fibroblastic cell lines. The corresponding dose-effect curve is of linear shape and shows a “shoulder” as it is observed for repair-competent cells (Fig. 1). The analysis of DSB induction and repair after exposure to X-rays using the γ -H2AX

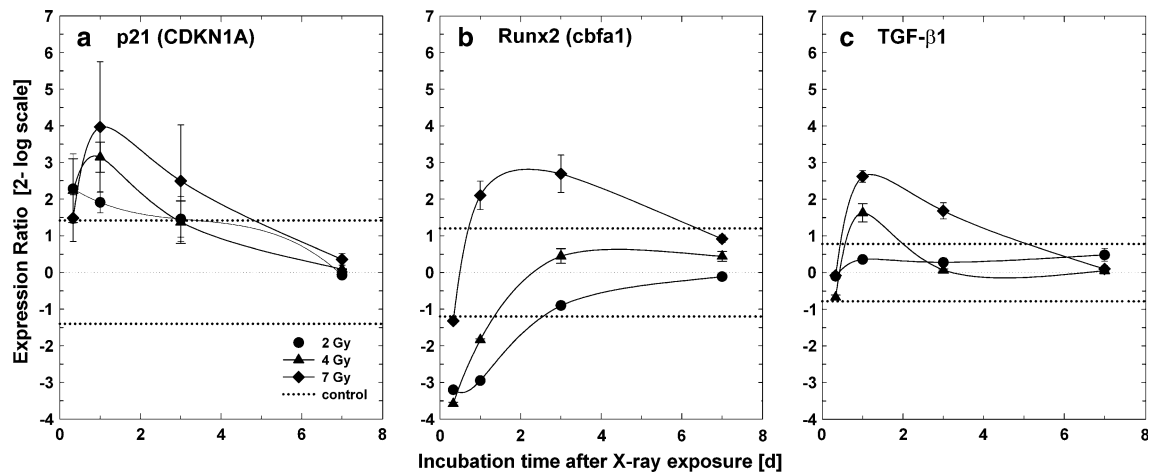


Fig. 5 Gene expression profiles of the transcription factor p21 (CDKN1A) and the bone-specific marker genes Runx2 and TGF- β 1. OCT-1 cells were exposed to X-rays (150 kV, 16 mA) and incubated for the indicated time points. Target gene expressions were normal-

ized against the expression of the optimal combination of the house-keeping genes B2M, HPRT and TBP using the BestKeeper software (Pfaffl et al. 2004). Dotted lines represent the standard deviation of all untreated samples

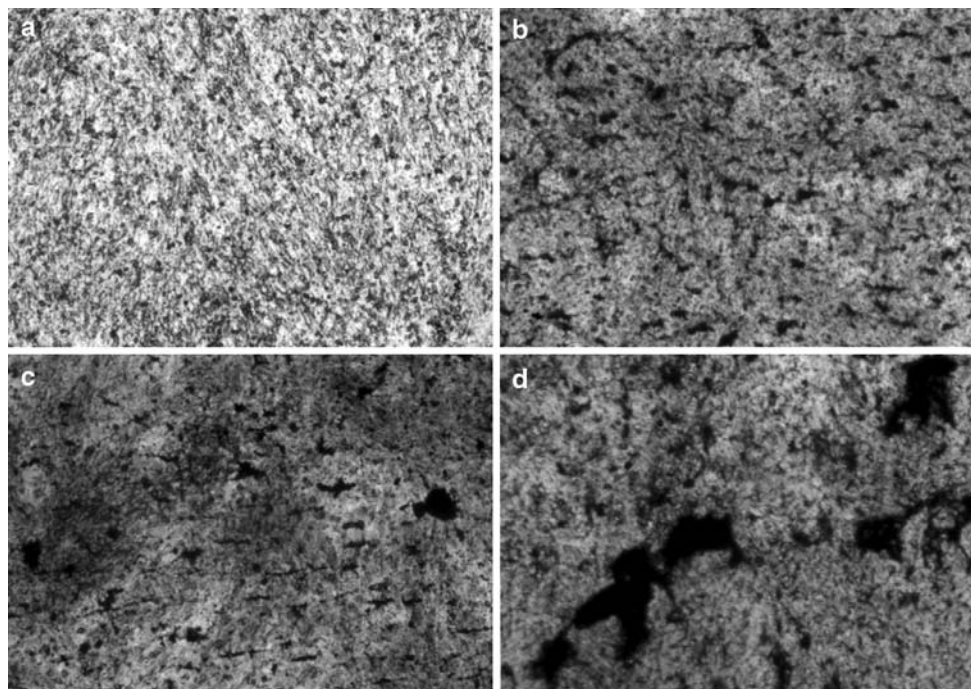


Fig. 6 Differentiation of OCT-1 cells 14 days after irradiation with 0 Gy (a), 2 Gy (b), 4 Gy (c) and 7 Gy (d): Cells were grown to confluence and stained according to von Kossa for extracellular deposited

calcium thereby visualizing mineralized bone nodules (black). Pictures were taken with a 5 \times objective magnification

immune staining technique reveals the repair competence for OCT-1 cells. About 36 ± 5.5 foci could be detected shortly after exposure to 1 Gy, a foci number that is well accepted for DSB induced per Gy in human fibroblasts (Rothkamm and Löbrich 2002; Rothkamm and Löbrich 2003). DNA repair kinetics of murine osteoblasts, as analyzed by time-dependent decay of γ -H2AX foci, is comparable to repair kinetics measured in fibroblasts.

It has been well documented that ionizing radiation induces DSB and activates checkpoints to block cells in G1 and G2 phase of the cell cycle. Cell cycle arrests are either resolvable after a certain repair period or are permanent when DNA repair is insufficient.

Cell proliferation is therefore a fundamental biological activity that is regulated through many gene products, including cyclin-dependent kinases (CDKs), enzymes for

DNA replication and repair, enzymes for chromatin condensation and segregation, proto-oncogenes and tumor suppressor genes (Abraham 2001). Many cell cycle regulators undergo dramatic changes in levels of expression and activity to propel or regulate progression through the cell division cycle (Cho et al. 2001). Identification of cell cycle-regulated genes will facilitate understanding of not only normal biological processes during cell division but also mechanisms of pathologic response to environmental toxicants. In the present study, we evaluated the expression of the CDK-inhibitor p21. The up-regulation of p21 early after exposure to IR was closely connected with the development of a G2 cell cycle arrest. After exposure to 2–7 Gy of X-rays, OCT-1 cells show a stringent G2-arrest 8 h after irradiation, which is resolved after 24 h for the cells irradiated with 2 Gy (Fig. 4). When cells were treated with doses of 4 and 7 Gy, they re-entered the cell cycle after 24 h or even later. The transcriptional regulation of cell cycle-regulated genes may be closely related to checkpoint functions upon DNA damage.

Cells harboring X-ray-induced irreparable DNA damage are programmed to die. Survival strategies to overcome the fact that the integrity of the genome is not maintained for cells with heavily damaged DNA include either accelerated senescence (Suzuki et al. 2001) or the initiation of premature terminal differentiation, which was frequently observed in human fibroblasts (Herskind et al. 2000; Herskind and Rodemann 2000; Fournier et al. 2001). As the relationship between cell cycle checkpoint function and differentiation has not been systematically studied in osteoblastic cells, we analyzed the relation between cell cycle progression and transcriptional regulation of gene expression by quantitative real-time PCR. Of interest in this respect are the bone-specific transcription factor Runx2 and the $\beta 1$ isoform of TGF- β .

Runx2 is an essential parameter for osteogenesis, and its absence is associated with severe bone abnormalities (Otto et al. 1997). Its expression indicates the osteogenic commitment of cells. The early X-ray-induced up-regulation of this osteoblast-specific key transcription factor correlates well with the up-regulation of the of cell cycle checkpoint regulator p21. The same is true for the expression of the $\beta 1$ isoform of TGF- β that has widespread activity in many essential cellular functions, ranging from control of cell cycle progression to the regulation of extracellular matrix production (Bonewald 1999; Croucher and Russell 1999). Results with fibroblasts (Herskind et al. 2000) indicate its role in terminal differentiation in radiation-induced fibrosis and imply that the progenitor population surviving radiation might be more prone to terminal differentiation than non-irradiated progenitor cells. Our results with the osteoblast progenitor cell line OCT-1 suggest that there is a link between exposure to ionizing radiation and osteoblastic

differentiation. Such a premature terminal differentiation of the bone-forming precursor cells is of special interest for radiotherapy of children and young adults. The up-regulation of differentiation-related genes in osteoblasts such as Runx2 is tightly coupled with down-regulation of genes related to proliferation. This up- and down-regulation of differentiation- and proliferation-related genes was followed by deposition of bone-forming extracellular matrix and generation of bone nodules in a dose-dependent manner.

Further experiments are certainly needed to uncover the complex interrelationship between different maturation stages of cells in the bone osteoblastic lineage and their radiation sensitivity. Such experiments that compare cell lines of various differentiation capacities in terms of expression of bone-specific marker genes with a sensitive detection method like quantitative polymerase chain reaction (qPCR) technique are currently being performed.

Acknowledgments The authors would like to thank Dr. D. Chen, University of Texas, San Antonio, USA for providing the OCT-1 cell line used in this work.

References

- Abraham RT (2001) Cell cycle checkpoint signaling through the ATM and ATR kinases. *Genes Dev* 15:2177–2196
- Alliston T, Choy L, Ducey P, Karsenty G et al (2001) TGF-beta-induced repression of CBFA1 by Smad3 decreases cbfa1 and osteocalcin expression and inhibits osteoblast differentiation. *EMBO J* 20:2254–2272
- Arnold M, Kummermehr J, Trott KR (1995) Radiation-induced impairment of osseous healing quantitative studies using a standard drilling defect in rat femur. *Radiat Res* 143:77–84
- Aubin JE (1998) Advances in the osteoblast lineage. *Biochem Cell Biol* 76:899–910
- Aubin JE, Liu F, Malaval L, Gupta AK (1995) Osteoblast and chondroblast differentiation. *Bone* 17(2 Suppl):77–83
- Augat P, Simon U, Liedert A, Claes L (2005) Mechanics and mechanobiology of fracture healing in normal and osteoporotic bone. *Osteoporos Int* 16(Suppl 2):36–43
- Bonewald LF (1999) Regulation and regulatory activities of transforming growth factor beta. *Crit Rev Eukaryot Gene Expr* 9:33–44
- Chen D, Chen H, Feng JQ, Windle JJ et al (1995) Osteoblastic cell lines derived from a transgenic mouse containing the osteocalcin promoter driving SV40 T antigen. *Molec Cell Differ* 3:193–212
- Chentoufi J, Hott M, Lamblin D, Buc-Caron MH et al (1993) Kinetics of in vitro mineralization by an osteogenic clonal cell line (C1) derived from mouse teratocarcinoma. *Differentiation* 53:181–189
- Cho RJ, Huang M, Campbell MJ, Dong H et al (2001) Transcriptional regulation and function during the human cell cycle. *Nat Genet* 27:48–54
- Croucher PI, Russell RG (1999) Growth Factors. In: Seibel MJ, Robins SP, Bilezikian JP (eds) *Dynamics of bone and cartilage metabolism*. Academic Press, San Diego, pp 453–464
- Dare A, Hachisu R, Yamaguchi A, Yokose S et al (1997) Effects of ionizing radiation on proliferation and differentiation of osteoblast-like cells. *J Dent Res* 76:658–664
- Ducey P, Zhang R, Geoffrey V, Ridall AL et al (1997) Osf2/Cbfa1: a transcriptional activator of osteoblast differentiation. *Cell* 89:747–754

- Dudziak ME, Saadeh PB, Mehrrara BJ, Steinbrech DS et al (2000) The effects of ionizing radiation on osteoblast-like cells in vitro. *Plast Reconstr Surg* 106:1049–1061
- Erguen H, Howland WJ (1980) Postirradiation atrophy of mature bone. *CRC Crit Rev Diagn Imaging* 12:225–243
- Fleige S, Pfaffel MW (2006) RNA integrity and the effect on the real-time qRT-PCR performance. *Mol Aspects Med* 27:126–139
- Fournier C, Scholz M, Weyrather WK, Rodemann HP et al (2001) Changes of fibrosis-related parameters after high- and low-LET irradiation of fibroblasts. *Int J Radiat Biol* 77:713–722
- Goldwein JW (1991) Effects of radiation therapy on skeletal growth in childhood. *Clin Orthop Relat Res* 262:101–107
- Harada H, Tagashira S, Fujiwara M, Ogawa S et al (1999) Cbfa1 isoforms exert functional differences in osteoblast differentiation. *J Biol Chem* 274:6972–6978
- Hayflick L (1965) The limited in vitro lifetime of human diploid cell strains. *Exp Cell Res* 37:614–636
- Herskind C, Rodemann HP (2000) Spontaneous and radiation-induced differentiation of fibroblasts. *Exp Gerontol* 35:747–755
- Herskind C, Johansen J, Bentzen SM, Overgaard M et al (2000) Fibroblast differentiation in subcutaneous fibrosis after postmastectomy radiotherapy. *Acta Oncol* 39:383–388
- Hopewell JW (2003) Radiation-therapy effects on bone density. *Med Pediatr Ocol* 41:208–211
- Hug O, Kellerer AM (1966) *Stochastik der Strahlenwirkung*. Springer, Berlin, Heidelberg, New York
- Jacobsson M, Jönsson A, Albrektsson T, Turesson L (1985) Alterations in bone regenerative capacity after low gamma irradiation. A quantitative study. *Scand J Plast Reconstr Surg* 19:231–236
- Jacobsson M, Kålebo P, Albrektsson T, Turesson L (1986) Provoked reptives healing of mature bone tissue following irradiation. A quantitative investigation. *Acta Radiol Ocol* 25:57–62
- Kanaan RA, Kanaan LA (2006) Transforming growth factor beta 1, bone connection. *Med Sci Monit* 12:164–169
- Kern B, Shen J, Starbuck M, Karsenty G (2001) Cbfa1 contributes to the osteoblast specific expression of type I collagen genes. *J Biol Chem* 276:7101–7107
- Komori T (2006) Regulation of osteoblast differentiation by transcription factors. *J Cell Biochem* 99:1233–1239
- Komori T, Yagi H, Nomura S, Yamaguchi A et al (1997) Targeted disruption of Cbfa1 results in a complete lack of bone formation owing to maturational arrest of osteoblasts. *Cell* 89:755–764
- Langdahl BL, Carstens M, Stenkjaer L, Eriksen EF (2003) Polymorphism in the transforming growth factor beta 1 gene and osteoporosis. *Bone* 32:297–310
- Mass P, Hoffmann K, Gambichler T, Altmeyer P et al (2003) Premature keratinocyte death and expression of marker proteins of apoptosis in human skin after UVB exposure. *Arch Dermatol Res* 295:71–79
- Nolan T, Hands RE, Bustin SA (2006) Quantification of mRNA using real-time RT-PCR. *Nat Protoc* 1(3):1559–1582
- Otto F, Thornell AP, Crompton T, Denzel A et al (1997) Cbfa1, a candidate gene for cleidocranial dysplasia syndrome, is essential for osteoblast differentiation and bone development. *Cell* 89:765–771
- Pfaffl MW (2001) A new mathematical model for relative quantification in real-time RT-PCR. *Nucl Acids Res* 29:e45. doi:10.1093/nar/29.9.e45
- Pfaffl MW, Horgan GW, Dempfle L (2002) Relative expression software tool (REST) for group-wise comparison and statistical analysis of relative expression results in real-time PCR. *Nucl Acids Res* 30(9):e36. doi:10.1093/nar/30.9.e36
- Pfaffl MW, Tichopad A, Prgomet C, Neuvians TP (2004) Determination of stable housekeeping genes, differentially regulated target genes and sample integrity: BestKeeper–Excel-based tool using pair-wise correlations. *Biotechnol Lett* 26(6):509–515
- Probert JC, Parker BR (1975) The effects of radiation therapy on bone growth. *Radiology* 114:155–162
- Rasmussen R (2001) Quantification of the light cyclase. In: Meuer S, Wittwer C, Nakagawara K (eds) *Rapid cycle real-time PCR, methods and applications*. Springer, Heidelberg, ISBN 3-540-66736-9:21–34
- Roberts AB, Sporn MB (1993) Physiological actions and clinical applications of transforming growth factor-beta (TGF-beta). *Growth Factors* 8:1–9
- Rodemann HP, Bayreuther K, Francz PI, Dittmann K et al (1989) Selective enrichment and biochemical characterization of seven human skin fibroblasts cell types in vitro. *Exp Cell Res* 180:84–93
- Rogakou EP, Pilch DR, Orr AH, Ivanova VS et al (1998) DNA double-stranded breaks induce histone H2AX phosphorylation on serine 139. *J Biol Chem* 273:5858–5868
- Rothkamm K, Löbrich M (2002) Misrepair of radiation-induced DNA double-strand breaks and its relevance for tumorigenesis and cancer treatment (review). *Int J Oncol* 21:433–440
- Rothkamm K, Löbrich M (2003) Evidence for a lack of DNA double-strand break repair in human cells exposed to very low X-ray doses. *Proc Natl Acad Sci USA* 100:5057–5062
- Sams A (1965) The effect of 2000 r of X-rays on the acid and alkaline phosphatase of mouse tibiae. *Int J Radiat Biol Relat Stud Phys Chem Med* 10:123–140
- Sowa H, Kaji H, Yamaguchi T, Sugimoto T et al (2002) Smad3 promotes alkaline phosphatase activity and mineralization of osteoblastic MC3T3–E1 cells. *J Bone Miner Res* 17:1190–1199
- Stein GS, Lian JB (1993) Molecular mechanism mediating proliferation/differentiation interrelationships during progressive development of the osteoblast phenotype. *Endocr Rev* 14:424–442
- Strewler GJ (2004) Decimal point-osteoporosis therapy at the 10-year mark. *N Engl J Med* 350:1172–1174
- Suzuki K, Mori I, Nakayama Y, Miyakoda M et al (2001) Radiation-induced senescence-like growth arrest requires TP53 function but not telomere shortening. *Radiat Res* 155:248–253
- Szymczyk KH, Shapiro IM, Adams CS (2004) Ionizing radiation sensitizes bone cells to apoptosis. *Bone* 34:148–156
- Tonna EA, Pavelec M (1970) Changes in the proliferative activity of young and old mouse skeletal tissues following Co60 whole-body irradiation. *J Gerontol* 25:9–16
- Vandesompele J, De Preter K, Pattyn F, Poppe B et al (2002) Accurate normalization of real-time quantitative RT-PCR data by geometric averaging of multiple internal control genes. *Genome Biol* 3:34
- Zhou T, Chou J, Mullen TE, Elkon R et al (2007) Identification of primary transcriptional regulation of cell cycle-regulated genes upon DNA damage. *Cell Cycle* 6:972–981
- zur Nieden NI, Kempka G, Ahr HJ (2003) In vitro differentiation of embryonic stem cells into mineralized osteoblasts. *Differentiation* 71:18–27